Psychological Medicine, 2001, **31**, 1425–1435. © 2001 Cambridge University Press
DOI: 10.1017/S0033291701004706 Printed in the United Kingdom

Distributed grey and white matter deficits in hyperkinetic disorder: MRI evidence for anatomical abnormality in an attentional network

S. OVERMEYER, E. T. BULLMORE,[1] J. SUCKLING, A. SIMMONS, S. C. R. WILLIAMS, P. J. SANTOSH AND E. TAYLOR

From the Institute of Psychiatry and Guy's, King's and St Thomas's School of Medicine, London; and Department of Psychiatry, University of Cambridge, Cambridge

ABSTRACT

Background. Previous neuroimaging studies of children with attention deficit hyperactivity disorder (ADHD) have demonstrated anatomic and functional abnormalities predominantly in frontal and striatal grey matter. Here we report the use of novel image analysis methods, which do not require prior selection of regions of interest, to characterize distributed morphological deficits of both grey and white matter associated with ADHD.

Methods. Eighteen children with a refined phenotype of ADHD, who also met ICD-10 criteria for hyperkinetic disorder (mean age 10·4 years), and 16 normal children (mean age 10·3 years) were compared using magnetic resonance imaging. The groups were matched for handedness, sex, height, weight and head circumference. Morphological differences between groups were estimated by fitting a linear model at each voxel in standard space, applying a threshold to the resulting voxel statistic maps to generate clusters of spatially contiguous suprathreshold voxels, and testing cluster 'mass', or the sum of suprathreshold voxel statistics in each 2D cluster, by repeated random resampling of the data.

Results. The hyperkinetic children had significant grey matter deficits in right superior frontal gyrus (Brodmann area (BA) 8/9), right posterior cingulate gyrus (BA 30) and the basal ganglia bilaterally (especially right globus pallidus and putamen). They also demonstrated significant central white matter deficits in the left hemisphere anterior to the pyramidal tracts and superior to the basal ganglia.

Conclusions. This pattern of spatially distributed grey matter deficit in the right hemisphere is compatible with the hypothesis that ADHD is associated with disruption of a large scale neurocognitive network for attention. The left hemispheric white matter deficits may be due to dysmyelination.

INTRODUCTION

Attention deficit hyperactivity disorder (ADHD) is characterized by inattentiveness, distractibility, hyperactivity, associated emotionality and apparent intrusiveness or destructiveness arising from impulsivity. Hyperkinetic disorder (HD) is a narrower diagnosis and is a subgroup of ADHD with different implications from those of other disturbances such as conduct disorder (Taylor *et al.* 1991, 1996). Inattention is a required criterion for HD but not for ADHD; children with HD should correspond to the combined attention deficit/hyperactivity subtype of ADHD (American Psychiatric Association, 1994), as well as meeting stricter criteria for the pervasiveness of the disorder across situations and the absence of other psychiatric

[1] Address for correspondence: Professor Edward T. Bullmore, University of Cambridge, Department of Psychiatry, Addenbrooke's Hospital, Cambridge CB2 2QQ.

disorders such as anxiety and depressive disorders (World Health Organization, 1993). Hyperkinetic disorder therefore corresponds closely to the refined phenotype of ADHD recommended for biological study by Swanson *et al.* (1998). Children with HD are at considerable developmental risk and have high rates of language and motor delays.

Researchers interested in the biological basis of ADHD have focused on the interactions of the prefrontal cortex with the caudate nucleus (Lou *et al.* 1989; Hynd *et al.* 1993; Roeltgen & Schneider, 1994), and the brainstem's dopaminergic and noradrenergic systems (Shaywitz *et al.* 1978). Global brain volume measured using MRI has been shown to be about 5% smaller in children with ADHD, compared to comparison children (Castellanos *et al.* 1996; Filipek *et al.* 1997). Children with ADHD seem also to have impaired metabolism in frontal regions (Lou *et al.* 1984, 1989; Amen *et al.* 1993; Zametkin *et al.* 1993; Sieg *et al.* 1995) and a smaller right prefrontal lobe (Hynd *et al.* 1990; Castellanos *et al.* 1996; Casey *et al.* 1997). The right prefrontal white matter appears to be specifically diminished in children with ADHD, which may be attributable to neurodevelopmental delay of the right frontal lobe (Castellanos *et al.* 1996).

On the basis of these and other data, several researchers have hypothesized a right frontostriatal deficit in children with ADHD (Lou *et al.* 1984, 1989, 1990; Castellanos *et al.* 1996; Casey *et al.* 1997). Filipek *et al.* (1997) have recently developed this hypothesis further, by conceptualizing different neural networks for selective attention, vigilance and executive functions. They reported smaller volumes of the right prefrontal cortex and supplementary motor area (components of a vigilance network), and mid-anterior cingulate gyrus and caudate nucleus (components of an executive network). Casey *et al.* (1997) have reported a significant positive correlation between performance scores on inhibition tasks and the volumes of the cingulate gyri, the right caudate nucleus and the globus pallidus. Castellanos *et al.* (1996) have also demonstrated smaller volumes of the same areas, in a sample of 57 male children and adolescents with ADHD; although, in a more recent study of girls with ADHD, Castellanos *et al.* (2001) found less salient abnormalities in frontal and striatal structure, especially after controlling the case–control comparison for effects of verbal IQ. Filipek *et al.* (1997) and Hynd *et al.* (1993) reported smaller volumes of the left caudate nucleus in children with ADHD. Regions of the corpus callosum, which are related to the superior parietal lobules, the inferior parietal lobules, angular gyrus and visual association areas have also been reported to be decreased in volume (Hynd *et al.* 1991; Semrud-Clikeman *et al.* 1994; Lyoo *et al.* 1996). Rubia *et al.* (1999) using functional MRI have reported reduced activation of right medial frontal cortex in two motor control tasks, and reduced activation of right ventrolateral prefrontal cortex and left caudate nucleus during a (stop) motor inhibition task.

Despite numerous neuroimaging studies being undertaken in children with ADHD (DSM-IV), none has specifically investigated the hyperkinetic disorder subtype. Even though some studies have included children with symptoms pervasive across situations, they would still differ from the ICD-10 concept of HD. Here we have investigated this narrowly defined, relatively homogenous group for the first time using neuroimaging. As a comparison group we chose the healthy siblings of children with hyperkinetic disorder. The reason for this choice was to provide a more rigorous comparison than is provided by the more usual design of comparison with volunteers from the general population. It is in principle possible that any changes in the brain in hyperkinetic subjects may reflect, not a causal abnormality, but a confounding abnormality of the environment. Physical adversity such as exposure to lead or nicotine, and psychological influences such as an unstimulating environment, could be more common in the families of children with hyperkinetic disorder, and could lead to alterations of brain structure and function, yet not be part of the pathogenesis of the disorder. We therefore wished to control for non-specific environmental effects that might be common to both patients with HD and the siblings of patients with HD.

We hypothesized that neuroanatomical abnormality in children with HD would be distributed throughout components of a large scale neurocognitive network normally subserving attention. To test this hypothesis without imposing the constraints entailed by prior selection of a few regions of interest, we applied

novel methods for image analysis that allowed us to examine both grey and white matter morphology over the whole brain.

METHOD

Subjects

Fifteen boys and three girls with a refined diagnosis of ADHD (aged between 8–13 years) were selected through a multi-stage procedure. All had been referred for specialist neuropsychiatric evaluation because of problems of inattentiveness, overactivity and/or impulsiveness. Systematic parental interview and psychiatric interview with the child were carried out (University of London, Institute of Psychiatry, 1987). Full-scale, Verbal and Performance IQs were assessed using the Wechsler Intelligence Scale for Children-Revised (WISC-R; Wechsler, 1974).

Behavioural, historical and psychometric data were reviewed independently by two child psychiatrists. Twenty-four subjects with ADHD were judged by both psychiatrists to meet criteria for attention deficit disorder with hyperactivity (ADHD, DSM-IV) and were initially enrolled in this study. Six could not remain still enough in the scanner because of anxiety. As recommended by Swanson *et al*. (1998), all 18 of the remaining patients met criteria for the refined phenotype of ADHD, mixed type, without co-morbid anxiety or mood disorder or learning disability; and these are the cases reported here. All 18 also met the World Health Organization criteria for hyperkinetic disorder and had a minimum full-scale IQ of 70; one patient had concurrent dyslexia, two had oppositional defiant disorder and two had conduct disorder. These cases were not excluded (and are not usually excluded from the refined phenotype) because oppositionality, defiance and conduct problems were considered to be complications of the hyperkinetic disorder. Sixteen of the 18 patients received methylphenidate for at least 1 year before the MRI scanning, one subject desipramine, and one subject D-amphetamine.

Comparison group

Fifteen age-matched male comparison subjects, and one female comparison subject (aged 7–14 years) who were healthy siblings of children attending the out-patient Hyperkinetic Clinic at the Child Psychiatry Department, Maudsley Hospital, London, entered the study. Only four were siblings of the subjects; the other comparison subjects were siblings of other children who had met criteria for ADHD at the same clinic. In order to justify the linking of morphological differences to the pathophysiology of ADHD, one should rule out the existence of similar brain morphology in close relatives of subjects with ADHD. If the morphometric measures of children with ADHD and phenotypically normal siblings of children with ADHD do not differ, then the ADHD phenotype may be mediated through other mechanisms. All subjects were attending normal school and were free of problems of inattentiveness, overactivity and/or impulsiveness. None had been referred for assessment or treatment of any psychological problem.

In order to check that the comparison group were indeed free of hyperactivity, all received the Parental Account of Children's Symptoms interview, which is a standardized, reliable, investigator-based interview measure for the recording of symptoms of hyperactivity, defiance and over-emotionality (PACS; Taylor *et al*. 1991). Cut-offs have been validated in clinical and epidemiological studies; a score above 0·9 indicates the probable presence of hyperactive behaviour. All comparison subjects scored under

Table 1. *Demographic and clinical characteristics of the sample*

	Hyperkinetic group Mean (S.D.) $N = 18$	Comparison group Mean (S.D.) $N = 16$	t (df = 33)	P
Age (years)	10·4 (1·7)	10·3 (2·2)	0·10	0·92
IQ (WISC-R)	99·0 (14·9)			
Head circumference (cm)	53·9 (1·9)	54·2 (3·1)	−0·25	0·81
Weight (kg)	34·3 (8·1)	40·3 (18·9)	−1·23	0·23
Height (cm)	140·8 (9·5)	143·6 (14·6)	−0·67	0·51
Conners' rating scale	24·3 (3·1)	5·9 (6·9)	10·26	< 0·000
Handedness	7 left (47%)	1 left (6%)	−3·52	0·001

0·9 (mean 0·17, S.D. 0·27). One of the 16 comparison subjects met criteria for oppositional defiant disorder (ODD) according to the PACS, but no other diagnosis could be given. The ODD child had a PACS hyperactivity score of 0·88 and was below the cut-off score for possible hyperactive behaviour.

Demographic and clinical characteristics of the samples are summarized in Table 1. There were no significant differences between groups in terms of age, head circumference, weight or height; but there were significantly more left-handed subjects in the hyperkinetic group. The difference in handedness (examined by the test of Soper *et al*. (1987)) may be a manifestation of a neurodevelopmental abnormality in this severely affected ADHD group. The current hyperkinetic behaviour was assessed using the screening instrument of Conners' scale, where the cut-off score is 15 for children with ADHD (Goyette *et al*. 1978). The significant difference reflects the different hyperkinetic behaviour of the two samples.

Written informed consent by the parents was obtained after the experimental investigation and interviews were fully explained to the parents; consent was also obtained from the children themselves. It was explained to the children and parents that MRI has two possibly alarming aspects: first it was noisy, and second it might induce claustrophobic anxiety. The children were always able to speak to the investigators and their parents and to withdraw from the study at any time without giving a reason. The study was approved by the Ethical Committee of the Bethlem Royal and Maudsley NHS Hospital Trust.

MRI data acquisition

Structural data were acquired at 1.5 Tesla from all subjects using a General Electric Signal System (GE, Milwaukee, WI, USA). A coronal localizer image was initially used to prescribe acquisition of a dual echo, fast spin echo dataset in the sagittal plane parallel to the inter-hemispheric fissure: TR = 4 s, TE1 = 20 ms, TE2 = 100 ms, number of data averages = 1. A pair of proton density (PD) and T2 weighted images were thus acquired, using a flow compensation scheme, at each of 50 interleaved, 3 mm thick slice positions. The field of view was 22 cm and the in-plane resolution was 0·86 mm. These acquisition parameters were chosen, based on simulated MRI data, to optimize the images for subsequent segmentation (Simmons *et al*. 1996). Head movement was limited by foam padding within the head coil and a restraining band across the forehead.

Since many of the subjects and parents were anxious about the unknown MRI procedure, a film was shown to them about the MRI environment before scanning. Parents were allowed into the scanning room, and both parents and children could watch an entertaining video during scanning (Overmeyer, 1996).

MRI data analysis

The first step in data analysis was segmentation of voxels representing extracerebral tissue, such as bone or skin. This was performed automatically by a computational algorithm using a linear scale-space set of features obtained from derivates of the Gaussian kernel; see Suckling *et al*. (1999) for further detail. Manual editing of the segmented images was necessary only to remove brainstem from the cerebral hemispheres and diencephalon.

The second step in analysis was probabilistic classification of each intracerebral voxel in the segmented images. A single operator (S. O.) selected a small training set of voxels representing each of the three main tissue classes from each MRI dataset. These training data were used to estimate the parameters of a polychotomous logistic discriminant function by maximum likelihood; and the trained or parameterized discriminant function was used to estimate the probability for each voxel belonging to each tissue class (Bullmore *et al*. 1995). As a result, a set of three maps was obtained from each MRI dataset, representing the voxel-wise probabilities of belonging to grey matter, white matter and cerebrospinal fluid (CSF) tissue classes. Based on prior results, we equate these probabilities to the proportional volumes of each tissue class in the often heterogeneous volume of tissue represented by each voxel (Bullmore *et al*. 1995). So, for example, if the probability of grey matter class membership was 0·8 for a given voxel, then it was assumed that 80% of the tissue represented by that voxel was grey matter. Given the voxel dimensions in millimetres, it was then straightforward to estimate the volume in millilitres of

Table 2. *Whole brain mean volume measurements (ml)*

Total volume	Hyperkinetic group ($N = 18$) Mean (S.D.)	Comparison group ($N = 16$) Mean (S.D.)	t (df = 33)	P
Brain	1385·0 (155·4)	1432·1 (152·6)	0·91	0·37
Grey matter	873·9 (122·5)	870·5 (109·1)	−0·09	0·93
White matter	432·9 (94·6)	471·6 (74·0)	1·36	0·19
CSF	78·7 (24·0)	90·0 (36·2)	1·1	0·28

Table 3. *Regions of significant grey matter volume deficit in the hyperkinetic group compared to the comparison group*

Cerebral region	BA	Side	N	x	y	z
Posterior cingulate gyrus	30	R	60	6	64	13
	31	R	38	9	53	29
	30/31	R	62	9	62	14
	30	R	46	12	61	13
Superior frontal gyrus	8	R	60	9	−36	47
	8	R	102	12	−35	45
Putamen/lateral globus pallidus		R	52	24	11	1
Putamen		R	124	27	−5	7
Putamen/medial globus pallidus		L	91	−12	−2	−5

BA, approximate Brodmann area; N, number of voxels comprising each 2D cluster; x,y,z, 3D coordinates (mm) in standard space (Talairach & Tournoux, 1988) for the voxel in each cluster representing maximum difference between groups.

grey matter, or any other tissue class, at each voxel. Summing over voxels, the tissue class volumes can be estimated over the whole brain. Intraoperator reliability for whole brain grey matter, white matter and CSF volume estimation in this way was excellent: intraclass correlation coefficient $> 0{\cdot}98$ for all tissue classes.

The third step in analysis was transformation of the three probability maps obtained from each individual dataset into a standard stereotactic space. To do this, a template image was first constructed by proportional rescaling of a subset of five PD-weighted images from different individuals selected of the comparison group. Using AFNI software (Cox, 1995) anatomical landmarks were identified, including the anterior and posterior commissures and lateral, superior and inferior convexities of the cerebral surface. The distances between landmarks were linearly rescaled to approximate each individual three-dimensional image to the reference brain depicted in a standard stereotactic atlas (Talairach & Tournoux, 1988). The five transformed images were then averaged to produce a single template image in standard space. The affine transformation, which minimized the sum of grey level differences between each individual's PD weighted image and the template image, was identified by the Fletcher–Davidon–Powell algorithm (Press *et al*. 1992; Brammer *et al*. 1997); and this individually estimated transformation matrix was applied in turn to each of that subject's three probability maps to register them in standard space.

An analysis of covariance (ANCOVA) model was then fitted at each voxel in standard space where there were $N = 34$ proportional volume (probability) estimates for each tissue class. The model is written below with grey matter proportional volume as the dependent variable:

$$G_{kj} = \mu + \alpha \mathrm{Group}_k + \beta \mathrm{Age}_{kj} + \gamma \mathrm{Hand}_{kj} + \delta \mathrm{Sex}_{kj} + \zeta \mathrm{Global}_{kj} + \varepsilon_{kj}. \quad (1)$$

Here G_{kj} denotes the proportional volume of grey matter estimated at a given voxel for the jth individual in the kth group; μ is the overall mean; $(\mu + \alpha \mathrm{Group}_k)$ is the mean of the kth group; and ε_{kj} is random variation. The covariates Age_{kj}, Hand_{kj}, Sex_{kj} and Global_{kj} denote the age, handedness, gender and global grey matter volume of the jth individual in the kth group.

This model was fitted at each intracerebral voxel of the observed data, with each class of proportional volume taken in turn as the dependent variable, to yield a set of three 'effect maps' of coefficient α divided by its standard error: $\alpha' = \alpha/\mathrm{SE}(\alpha)$. This model was also fitted 10 times at each voxel for each tissue class after random permutation of the elements of the factor coding group membership. This generated 10 randomized or permuted effect maps for each tissue class. Both observed and permuted effect maps were then thresholded such that if the

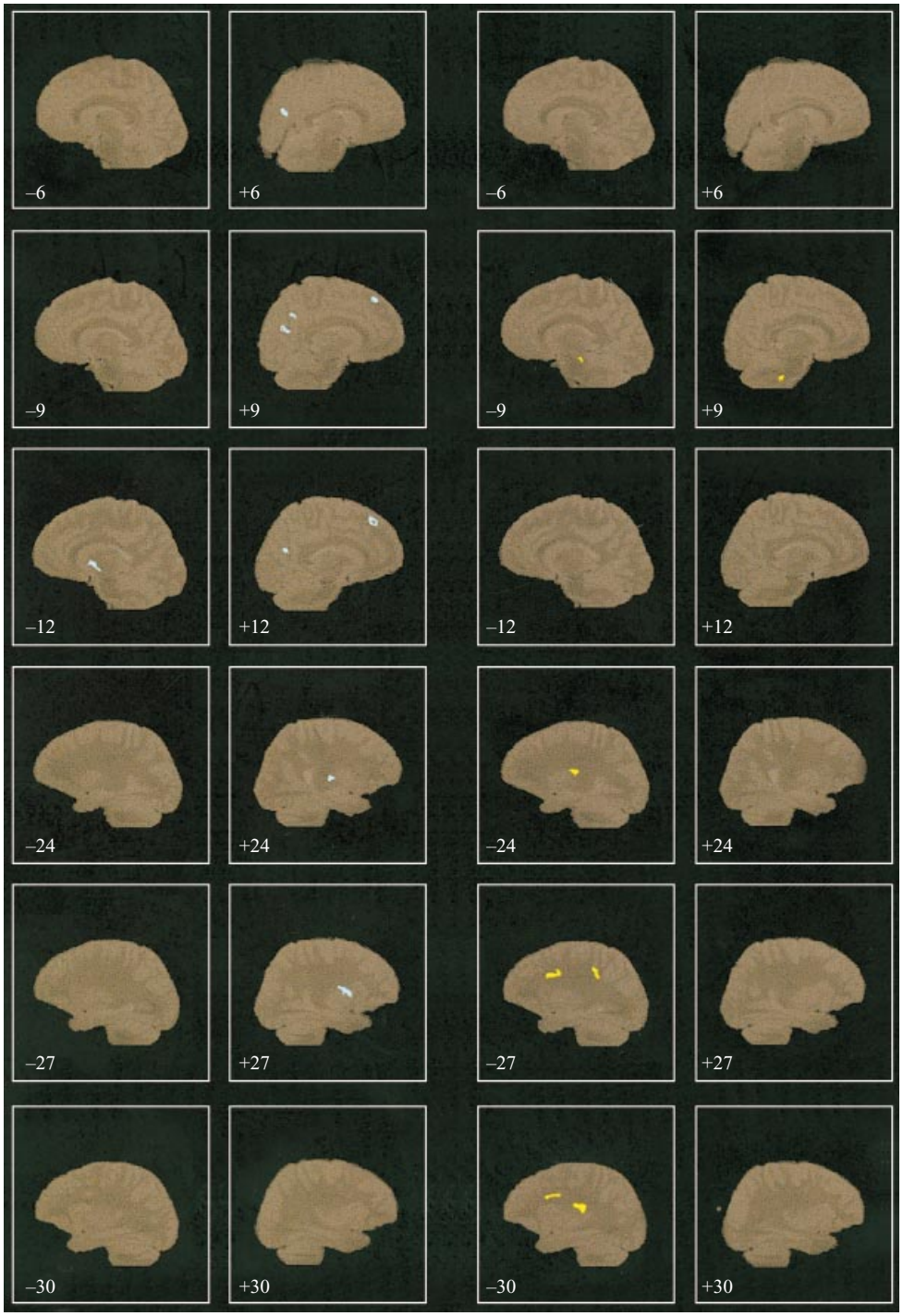

FIG. 1. Areas of grey and white matter deficit in 18 hyperkinetic children and adolescents compared to 16 comparison subjects. Blue voxels in the left hand pair of columns identify clusters of grey matter volume deficit (permutation test of 2D cluster mass; one-tailed $P = 0{\cdot}025$); yellow voxels in the right hand pair of columns identify clusters of white matter volume deficit (permutation test of 2D cluster mass; one-tailed $P = 0{\cdot}025$). The coloured voxels are superimposed on a proton density-weighted template image in standard

absolute value of α' was less than 1·96 the value of that voxel was set to zero and if the absolute value of α' was greater than 1·96 the value of that voxel was set to $\alpha' - 1{\cdot}96$ (that is, assuming a normal distribution, only the largest 5% of values were retained). This procedure generates several clusters of suprathreshold voxels that are spatially contiguous in-plane. The 'mass' of each two-dimensional cluster is the sum of its suprathreshold voxel statistics. Two-dimensional cluster mass was similarly measured in each of the 10 permuted effect maps generated for each tissue class. These measurements sample the permutation distribution of cluster mass under the null hypothesis of zero group difference in grey or white matter anatomy. The mass of each cluster in the observed effect maps was then tested against critical values obtained from the permutation distribution. This non-parametric or distribution free hypothesis testing procedure was adopted because there is considerable evidence from functional imaging that cluster level statistics, incorporating information about the spatial neighbourhood of each voxel, may be more sensitive than voxel test statistics (Poline & Mazoyer, 1993; Rabe-Hesketh *et al.* 1997); but theoretical distributions for cluster statistics may be intractable or of limited generalizability (Bullmore *et al.* 1999; Ashburner & Friston, 2000). Cluster level analysis also implies far fewer tests than voxel level analysis, meaning the multiple comparisons problem is less severe. Here we have used a cluster-wise one-tailed probability threshold $P < 0{\cdot}025$ for tests of 2D cluster mass. For greater procedural detail, and a comparative validation of nominal Type I error control by this method, see Bullmore *et al.* (1999).

RESULTS

Mean total brain volume and mean total volumes of grey matter, white matter and CSF are summarized for each group in Table 2. There was a 3·2% reduction of total brain volume, an 8·2% reduction of total white matter volume and a 12·5% reduction of total CSF volume, in the hyperkinetic group. None of these differences were statistically significant however.

Table 4. *Regions of significant white matter deficit in the hyperkinetic group compared to the comparison group*

Cerebral region	Side	*N*	*x*	*y*	*z*
	L	67	−30	−10	−24
	L	123	−30	21	−12
	L	113	−27	−9	−26
	L	27	−38	−28	79
	L	24	−14	−9	63
	L	9	−21	22	23
	R	9	28	41	39

N, number of voxels comprising each 2D cluster; *x*, *y*, *z*, 3D coordinates (mm) in standard space (Talairach & Tournoux, 1988) for the voxel in each cluster representing maximum difference between groups.

Anatomical regions demonstrating a significant difference between groups in grey matter proportional volume are listed in Table 3 and shown in Fig. 1. There were three main loci of regional deficit, all in the right hemisphere: medial superior frontal gyrus, posterior cingulate gyrus and retrosplenial cortex, and putamen and globus pallidus. There were also areas of reduced grey matter volume in the left globus pallidus.

Anatomical regions demonstrating a significant difference between groups in white matter proportional volume are listed in Table 4 and shown in Fig. 1. Most of the white matter volume deficits were located in the left hemisphere, rostral to the corticospinal projection from precentral gyrus and superior to the basal ganglia.

DISCUSSION

We have applied novel techniques of image analysis to estimate the volume of each tissue class represented by each voxel in each subject's MRI dataset; and then to identify spatial clusters of voxels that demonstrate a significant difference in grey or white matter volume between patient and comparison groups (Bullmore *et al.* 1995, 1999). The main advantage

space; the *x* coordinates of each slice in the coordinate system of Talairach & Tournoux (1988) are shown in the bottom left corner of each panel. Note that grey matter volume deficits are almost exclusively localized to right hemisphere regions (superior frontal gyrus, posterior cingulate gyrus and putamen/globus pallidus), whereas white matter volume deficits are mostly located superior to the left basal ganglia.

of this approach is that it has allowed us to identify neuroanatomical deficits associated with hyperkinetic disorder without restricting our attention to a few regions of interest (ROIs). We have therefore been able to demonstrate theoretically plausible abnormalities in posterior cingulate gyrus (which has not been adopted as a region of interest in previous imaging studies of ADHD), and in central white matter (which is not easy to parcel into regions of interest). The validity of these novel findings is supported by demonstration of associated abnormalities in right hemispheric prefrontal cortex and basal ganglia that were predicted by the existing literature.

One interpretation of this multi-regional pattern of right hemispheric grey matter deficit in hyperkinetic disorder is in terms of network models for attention. For example, Posner & Petersen (1990) identified an attentional system with an anterior component, comprising frontal and striatal regions, specialized for executive attention, and a posterior component, comprising parietal and posterior cingulate cortices, specialized for orientation and vigilance. Similarly, Mesulam (1990) described a right hemispheric neurocognitive network for spatially coordinated attention, which comprised frontal eyefields (approximate Brodmann area 8/6), posterior cingulate and retrosplenial cortices, posterior parietal cortex and basal ganglia. Here we have shown that three out of four of these anatomically interconnected areas demonstrate significant grey matter deficits in hyperkinetic children. Widespread anatomical disruption of attentional systems could plausibly determine the attention deficits associated with hyperkinetic disorder; but the pathogenetic mechanism responsible for generating such distributed pathological changes remains uncertain.

Hypodopaminergic modulation of frontal synapses by the basal ganglia may impair the normal age-related development of the grey matter (Rothenberger & Huther, 1997). It has also been reported that normal age-related changes in brain morphology are not seen in children with ADHD (Castellanos *et al*. 1994; Mataro *et al*. 1997). It is possible therefore that brain abnormalities in ADHD may be developmentally determined, and in this respect our finding of left anterior white matter deficits is interesting. The left hemisphere generally develops later than the right hemisphere, and anterior axonal tracts, projecting to or from frontal cortex, mature later than axonal tracts projecting to less recently evolved brain regions (Yakovlev & Lecours, 1969; Huttenlocher & Dabholkar, 1997). Relatively delayed brain development might therefore be indicated by abnormal or delayed myelination of left anterior white matter tracts in late childhood. Assuming that dysmyelination causes changes in local MR signal intensity that reduce the estimated proportion of white matter, this might explain our observation of left frontal white matter deficit in this group of hyperkinetic children.

It is interesting to compare our results to the recent study by Castellanos *et al*. (2001). These authors measured global and regional grey matter volumes in a sample of 50 girls with ADHD and 50 comparison subjects. They found a significant deficit in total cerebral volume of 3·9% in the patient group, which is comparable to the non-significant 3·2% deficit reported here: the difference in significance clearly reflects the greater power conferred by the larger sample in Castellanos *et al*. (2001). However, they did not find significant deficits in right frontal or striatal regions. This discrepancy with our results, and with the prior results of Castellanos *et al*. (1996), could have many possible explanations. For example our sample was predominantly male and the sample studied by Castellanos *et al*. (1996) was exclusively male, raising the possibility that gender has a pathoplastic effect on anatomical expression of ADHD. It is notable also that we studied a refined, relatively homogeneous subgroup of patients with hyperkinetic disorder, whereas the broader category of ADHD patients studied by Castellanos *et al*. (2001) may have included a greater variety of underlying anatomical abnormalities, potentially reducing the power of that study to detect regional deficits consistently expressed among members of the patient group. Finally, there are differences in morphometric methodology which may be relevant. Castellanos *et al*. (2001) used automated segmentation and normalization algorithms to measure grey matter volume in each of several previously defined frontal and subcortical regions of interest. We have also used computerized methods to segment and normalize the imaging data but we have then tested the null hypothesis of no difference

between cases and controls without any prior constraints on the anatomical expression of possible differences. Therefore, our method will be sensitive to detect a difference in anatomy that may be smaller than, or may cross the boundaries between, the regions of interest adopted *a priori* by cerebral parcellation schemes such as that used by Castellanos *et al.* (2001).

All methods of computational morphometry are relatively novel and it is important to consider the validity of these newer methods in relation to more traditional techniques of morphometry, such as manual delineation of the boundaries of an anatomical region of interest (ROI). The methods described here have previously been applied to analysis of structural images acquired from patients with chronic schizophrenia (Sigmundsson *et al.* 2001). These results were compared to the results of a meta-analysis of all prior imaging studies of schizophrenia using ROI morphometry (Wright *et al.* 2000). It was found that areas of grey matter deficit in medial and lateral temporal cortex in patients, and areas of relative grey matter excess in the basal ganglia, which were identified by Sigmundsson *et al.* (2001), were predicted by the ROI-based literature. Whereas abnormalities in insula and medial frontal cortex, which were also identified by Sigmundsson *et al.* (2001) but had not been predicted by the meta-analysis of studies using ROI morphometry (Wright *et al.* 2000), were located in brain areas that had simply not been adopted *a priori* as regions of interest by any eligible study in the previous literature. Another recent study has more directly compared these computational morphometric measures of grey matter deficit in patients with tuberous sclerosis to traditional, radiological counts of tubers and subependymal nodules (Ridler *et al.* 2001). It was shown that novel, computational measures of grey matter pathology were significantly (negatively) correlated with radiological indices of pathology in these patients. Additionally, we have carefully calibrated the performance of these algorithms by analysis of datasets in which we expect there to be no real anatomical difference between two groups of images and shown that the permutation-based techniques used here for inference on spatial statistics provide exact type 1 error control (Bullmore *et al.* 1999).

The current study has a number of limitations. First, the sample size is small, meaning there is a considerable risk of type 2 (false negative) error. This is evident in our failure to show a significant deficit in overall brain size, despite measuring a percentage deficit of comparable magnitude to the significant difference demonstrated by Castellanos *et al.* (2001) in a larger sample. It implies also that there may be other regional deficits of grey and/or white matter structure associated with ADHD than those we have described in this sample. Another limitation is that the patients differed from the comparison subjects not only in terms of hyperactivity but also in terms of handedness and exposure to stimulant medication. We have attempted to control the effects of handedness by including it as a factor in the linear model used to estimate group differences in grey and white matter at each voxel. The neuroanatomical effects of stimulant medication are not well known. However, it will clearly be important to replicate and extend these findings in larger samples and in samples of exclusively right-handed and drug-naive children with hyperkinetic disorder.

S.O. was supported by a European Fellowship awarded by the European Union Programme for the Training and Mobility of Researchers. E.T.B. was supported by the Wellcome Trust. This study was also supported by the Bethlem and Maudsley NHS Trust.

This paper was presented in a preliminary form at the 5th International Conference on Functional Mapping of the Human Brain, Düsseldorf, 22–26 June, 1999 and at the 11th International Congress of the European Society for Child and Adolescent Psychiatry, Hamburg, 15–19 September, 1999.

REFERENCES

Amen, D. G., Paldi, F. & Thisted, R. A. (1993). Brain SPECT imaging. *Journal of American Academy of Child & Adolescent Psychiatry* **32**, 1080–1081.

American Psychiatric Association (1994). *Diagnostic and Statistical Manual of Mental Disorders*, *4th edn*. American Psychiatric Association: Washington, DC.

Ashburner, J. & Friston, K. J. (2000). Voxel-based morphometry – the methods. *NeuroImage* **11**, 805–821.

Brammer, M. J., Bullmore, E. T., Simmons, A., Williams, S. C. R., Grasby, P. M., Howard, R. J., Woodruff, P. W. R. & Rabe-Hesketh, S. (1997). Generic brain activation mapping in fMRI: a nonparametric approach. *Magnetic Resonance Imaging* **15**, 763–770.

Bullmore, E. T., Brammer, M. J., Rouleau, G., Everitt, B. S., Simmons, A., Sharma, T., Frangou, R., Murray, R. M. & Dunn, G. (1995). Computerised brain tissue classification of magnetic

resonance images: a new approach to the problem of partial volume artefact. *NeuroImage* **2**, 133–147.

Bullmore, E. T., Suckling, J., Overmeyer, S., Rabe-Hesketh, S., Taylor, E. & Brammer, M. J. (1999). Global, voxel and cluster tests, by theory and permutation, for a difference between two groups of structural MR images of the brain. *IEEE Transactions on Medical Imaging* **18**, 32–42.

Casey, B. J., Castellanos, F. X., Giedd, J. N., Marsh, W. L., Hamburger, S. D., Schubert, A. B., Vauss, Y. C., Vaituzis, A. C., Dickstein, D. P., Sarfatti, S. E. & Rapoport, J. L. (1997). Implication of right frontostriatal circuitry in response inhibition and attention-deficit/hyperactivity disorder. *Journal of American Academy of Child & Adolescent Psychiatry* **37**, 374–383.

Castellanos, F. X., Giedd, J. N., Eckburg, P., Marsh, W. L., Vaituzis, A. C., Kaysen, D., Hamburger, S. D. & Rapoport, J. L. (1994). Quantitative morphology of the caudate nucleus in attention deficit hyperactivity disorder. *American Journal of Psychiatry* **151**, 1791–1796.

Castellanos, F. X., Giedd, J. N., Marsh, W. L., Hamburger, S. D., Vaituzis, A. C., Snell, J. W., Lange, N., Dickstein, D. P., Vauss, Y. C., Kaysen, D., Ritchie, G. F., Rajapakse, J. C. & Rapoport, J. L. (1996). Quantitative brain magnetic resonance imaging in attention-deficit/hyperactivity disorder. *Archives of General Psychiatry* **53**, 607–616.

Castellanos, F. X., Giedd, J. N., Berquin, P. C., Walter, J. M., Sharp, W., Tran, T., Vaituzis, A. C., Blumenthal, J. D., Nelson, J., Bastain, T. M., Zijdenbos, A., Evans, A. C. & Rapoport, J. L. (2001). Quantitative brain magnetic resonance imaging in girls with attention-deficit/hyperactivity disorder. *Archives of General Psychiatry* **58**, 289–295.

Cox, R. W. (1995). Analysis and visualisation of 3D fMRI data. *Proceedings of 3rd Scientific Meeting, Society of Magnetic Resonance* **2**, 834.

Filipek, P. A., Semrud-Clikeman, M., Steingard, R. J., Renshaw, P. F., Kennedy, D. N. & Biederman, J. (1997). Volumetric MRI analysis comparing subjects having attention-deficit hyperactivity disorder with normal controls. *Neurology* **48**, 589–601.

Goyette, C. H., Canners, C. K. & Ulrich, R. F. (1978). Normative data on revised Conners' parent and teacher rating scales. *Journal of Abnormal Child Psychology* **6**, 221–236.

Huttenlocher, P. R. & Dabholkar, A. S. (1997). Regional differences in synaptogenesis in human cerebral cortex. *Journal of Comparative Neurology* **387**, 167–178.

Hynd, G. W., Semrud-Clikeman, M., Lorys, A. R., Novey, E. S. & Eliopulos, D. (1990). Brain morphology in developmental dyslexia and attention deficit disorder/hyperactivity. *Archives of Neurology* **47**, 919–926.

Hynd, G. W., Semrud-Clikeman, M., Lorys, A. R., Novey, E. S., Eliopulos, D. & Lyytinen, H. (1991). Corpus callosum morphology in attention deficit-hyperactivity disorder: morphometric analysis of MRI. *Journal of Learning Disability* **24**, 141–l46.

Hynd, G. W., Hern, K. L., Novey, E. S., Eliopulos, D., Marshall, R., Gonzales, J. J. & Voeller, K. K. (1993). Attention deficit-hyperactivity disorder and asymmetry of the caudate nucleus. *Journal of Child Neurology* **8**, 339–347.

Lou, H. C., Henriksen, L. & Bruhn, P. (1984). Focal cerebral hypoperfusion in children with dysphasia and/or attention deficit disorder. *Archives of Neurology* **41**, 825–829.

Lou, H. C., Henriksen, L., Bruhn, P., Borner, H. & Nielsen, J. B. (1989). Striatal dysfunction in attention deficit and hyperkinetic disorder. *Archives of Neurology* **46**, 48–52.

Lou, H. C., Henriksen, L. & Bruhn, P. (1990). Focal cerebral dysfunction in developmental learning disabilities. *Lancet* **335**, 8–11.

Lyoo, I. K., Noam, G. G., Lee, C. K., Lee, H. K., Kennedy, B. P. & Renshaw, P. F. (1996). The corpus callosum and lateral ventricles in children with attention deficit hyperactivity disorder: a brain magnetic imaging study. *Biological Psychiatry* **40**, 1060–1063.

Mataro, M., Garcia-Sanchez, C., Junque, C., Estevez-Gonzalez, A. & Pujol, J. (1997). Magnetic resonance imaging measurement of the caudate nucleus in adolescents with attention-deficit hyperactivity disorder and its relationship with neuropsychological and behavioral measures. *Archives of Neurology* **54**, 963–968.

Mesulam, M.-M. (1990). Large-scale neurocognitive networks and distributed processing for attention, language, and memory. *Annals of Neurology* **28**, 597–613.

Overmeyer, S. (1996). Anxiety and coping of child psychiatric patients in magnetic resonance imaging. *Monatsschrift Kinderheilkunde* **144**, 1337–1341.

Poline, J. B. & Mazoyer, B. M. (1993). Analysis of individual positron emission tomography activation maps by detection of high signal-to-noise-ratio pixel clusters. *Journal of Cerebral Blood Flow & Metabolism* **13**, 425–437.

Posner, M. I. & Petersen, S. E. (1990). The attention system of the human brain. *Annual Review of Neuroscience* **13**, 25–42.

Press, W. H., Teukolsky, S. A., Vetterling, W. T. & Flannery, B. P. (1992). *Numerical Recipes in C: The Art of Scientific Computing*. Cambridge University Press: Cambridge.

Rabe-Hesketh, S., Bullmore, E. T. & Brammer, M. J. (1997). The analysis of functional magnetic resonance images. *Statistical Methods in Medical Research* **3**, 215–237.

Ridler, K., Bullmore, E. T., de Vries, P. J., Suckling, J., Barker, G. J., Meara, S. J. P., Williams, S. C. R. & Bolton, P. F. (2001). Widespread anatomical abnormalities of grey and white matter in tuberous sclerosis. *Psychological Medicine* **31**, 1437–1446.

Roeltgen, D. P. & Schneider, J. S. (1994). Task persistence and learning ability in normal and chronic low dose MPTP-treated monkeys. *Behavioral Brain Research* **60**, 115–124.

Rothenberger, A. & Huther, G. (1997). The role of psychosocial stressors in childhood for structural and functional brain development: neurobiological basis of developmental psychopathology. *Praxis der Kinderpsychologie und Kinderpsychiatrie* **46**, 623–644.

Rubia, K., Overmeyer, S., Taylor, E., Brammer, M. J., Williams, S. C. R., Simmons, A. & Bullmore, E. T. (1999). Hypofrontality in attention deficit hyperactivity disorder during higher-order motor control: a study with functional MRI. *American Journal of Psychiatry* **156**, 891–896.

Semrud-Clikeman, M., Filipek, P. A., Biederman, J., Steingard, R., Kennedy, D., Renshaw, P. & Bekken, K. (1994). Attention-deficit hyperactivity disorder: magnetic resonance imaging morphometric analysis of the corpus callosum. *Journal of American Academy of Child & Adolescent Psychiatry* **33**, 875–881.

Shaywitz, S. E., Cohen, D. J. & Shaywitz, B. A. (1978). The biochemical basis of minimal brain dysfunction. *Journal of Pediatrics* **92**, 79–87.

Sigmundsson, T., Suckling, J., Maier, M., Williams, S. C. R., Bullmore, E. T., Greenwood, K. E., Fukuda, R., Ron, M. A. & Toone, B. K. (2001). Structural abnormalities in frontal, temporal and limbic regions and interconnecting white matter tracts in schizophrenic patients with prominent negative symptoms. *American Journal of Psychiatry* **158**, 234–243.

Sieg, K. G., Gaffney, G. R., Preston, D. F. & Hellings, J. A. (1995). SPECT brain imaging abnormalities in attention deficit hyperactivity disorder. *Clinical Nuclear Medicine* **20**, 55–60.

Simmons, A., Arridge, S. R., Barker, G. J. & Williams, S. C. R. (1996). Simulation of MRI cluster plots and application to neurological segmentation. *Magnetic Resonance Imaging* **14**, 73–92.

Soper, H. V., Satz, P., Orsini, D. L., Van-Gorp, W. G. & Green, M. F. (1987). Handedness distribution in a residential population with severe or profound mental retardation. *American Journal of Mental Deficiency* **92**, 94–102.

Suckling, J., Brammer, M. J., Lingford-Hughes, A. & Bullmore, E. T. (1999). Removal of extracerebral tissues in dual echo magnetic resonance images via linear scale space features. *Magnetic Resonance Imaging* **17**, 246–257.

Swanson, J. M., Sergeant, J. A., Taylor, E., Sonuga-Barke, E. J., Jensen, P. S. & Cantwell, D. P. (1998). Attention-deficit hyperactivity disorder and hyperkinetic disorder. *Lancet* **351**, 429–433.

Talairach, J. & Tournoux, P. (1988). *Co-planar Stereotaxic Atlas of the Human Brain*. Thieme Medical Publishers: New York.

Taylor, E., Sandberg, S., Thorley, G. & Giles, S. (1991). *The Epidemiology of Childhood Hyperactivity: Maudsley Monographs* (*33*). Oxford University Press: Oxford.

Taylor, E., Chadwick, O., Heptinstall, E. & Danckaerts, M. (1996). Hyperactivity and conduct problems as risk factors for adolescent development. *Journal of American Academy of Child & Adolescent Psychiatry* **35**, 1213–1226.

Wechsler, D. (1974). *Wechsler Intelligence Scale for Children-Revised* (*WISC-R*). Psychological Corporation: New York.

World Health Organization (1993). *The ICD-10 Classification of Mental and Behavioural Disorders. Diagnostic Criteria for Research*. World Health Organization: Geneva.

Wright, I. C., Rabe-Hesketh, S., Woodruff, P. W. R., David, A. S., Murray, R. M. & Bullmore, E. T. (2000). Meta-analysis of regional brain volumes in schizophrenia. *American Journal of Psychiatry* **157**, 16–25.

Yakovlev, P. I. & Lecours, A. R. (1969). The myelogenetic cycles of regional maturation of the brain. In *Regional Development of the Brain in Early Life* (ed. A. Minkowski), pp. 3–70. Blackwell Scientific: Oxford.

Zametkin, A. J., Liebenauer, L. L., Fitzgerald, G. A., King, A. C., Minkunas, D. V., Herscovitch, P., Yamada, E. M. & Cohen, R. M. (1993). Brain metabolism in teenagers with attention-deficit hyperactivity disorder. *Archives of General Psychiatry* **50**, 333–340.